Lasers in Surgery and Medicine 20:416–425 (1997)

Intraocular Measurements of Pressure Transients Induced by Excimer Laser Ablation of the Cornea

Salvatore Siano, PhD,[1] Roberto Pini, PhD,[1]* Pier Giorgio Gobbi, PhD,[2] Renzo Salimbeni, PhD,[1] Matteo Vannini, PhD,[1] Francesco Carones, MD,[3] Giuseppe Trabucchi, MD,[3] and Rosario Brancato, MD[3]

[1]Quantum Electronic Institute, National Research Council, Florence, I-50127 Italy
[2]Laser Medicine Research, Scientific Institute H. S. Raffaele, Milan, I-20132 Italy
[3]Department of Ophthalmology and Visual Science, Scientific Institute H. S. Raffaele, University of Milan, Milan, I-20132 Italy

Background and Objective: **The evolution of pressure waves induced by argon-fluoride laser ablation of the cornea in the typical operative conditions of clinical laser keratectomy has been studied experimentally and analyzed.**
Materials and Methods: **Freshly enucleated porcine eyes were irradiated at a laser fluence of 180 mJ/cm² with various spot diameters in the range 1–6.5 mm. Pressure transients were detected by a fast rise time needle hydrophone inserted into the eyeball from the posterior pole and moved along the eye optical axis toward the cornea.**
Results: **Pressure peaks as high as 90 bar and of 50 ns pulse duration (FWHM) were measured in the anterior chamber. Observation of the pulse shape evolution during propagation put in evidence the onset of a marked rarefaction phase following the compressional spike, with intense negative peaks (up to –40 bar) located at increasing distances from the corneal surface for increasing spot diameters.**
Conclusions: **This behavior was explained by means of simplified models describing pressure pulse generation and diffraction effects occurring during its propagation. Implications to clinical procedures, as possible damages due to tissue stretching and cavitation formation, are also discussed. Lasers Surg. Med. 20: 416–425, 1997.** **© 1997 Wiley-Liss, Inc.**

Key words: argon-fluoride laser; photoacoustic waves; PRK

INTRODUCTION

Since the first proposals of excimer laser surgery of the cornea [1,2], very attractive features associated with UV laser ablation of biotissues have been recognized as the allowance of fine submicrometric control of the ablated layer due to the short penetration depth of the UV radiation into tissue and the absence of significant thermal side effects to the adjacent structures.

The study of physical and chemical mechanisms involved in this process has proceeded in the last decade in parallel with the observation and analysis of similar phenomena induced in organic polymers by the same UV laser radiation. In this respect, whereas the first studies attributed a primary role in material removal to direct bond-breaking of organic molecules by high energy UV photons [3–5] (namely, "ablative photodecomposition"), soon after it was recognized that thermal and mechanical aspects also had to be considered to account for the actually observed ablation thresholds and removal rates [6]. Recent studies have pointed out that the photochemical removal mechanism plays a fundamental role only in the ablation of organic polymers at 193

*Correspondence to: Dr. Roberto Pini, IEQ-CNR, Via Panciatichi 56/30, I-50127 Firenze, Italy.

Accepted for publication 16 July 1996.

© 1997 Wiley-Liss, Inc.

nm [7], whereas in most organic tissues, as well as in polymers irradiated at longer wavelengths, the dynamics of the interaction are mainly driven by thermal processes.

At present, the mechanisms responsible for the ablation of biotissue by UV lasers (and in general by pulsed lasers) can be very schematically classified by considering three main processes: (1) inertial (or pressure) confinement [8–10], (2) spallation [11], and (3) fast thermal vaporization [6,12]. The first two can explain tissue ablation occurring below the vaporization threshold, defined as the critical energy that induces phase transition in the irradiated volume of tissue. Worth noting, while calculating this volume, is that an effective penetration depth ($L = 1/\alpha_{eff}$) has to be considered, accounting for the nonlinear absorption effects induced by high power irradiation [13–15]. Plasma-mediated processes are not considered here because they concern laser intensities at least one order of magnitude greater than those typically employed in surgical procedures.

Whichever of the above is the removal mechanism, the studies devoted to surgical applications of pulsed laser ablation cannot neglect a careful analysis of the associated photoacoustic effects produced into tissue, which can be originated by thermoelastic expansion, by the recoil of fast material ejection, or by a combination of both, depending on the irradiation conditions.

In the specific case of corneal tissue ablation with 193 nm argon-fluoride (ArF) excimer lasers, the process of material removal can be considered in a first-order approximation as a fast thermal explosion driven mainly by water vaporization [6,12]. The explosive material ejection from the corneal surface originates an intense pressure transient propagating into the eye. In such a process, the typical pulse duration of ArF lasers (10–20 ns), much longer than the stress relaxation time of the cornea at 193 nm ($\tau_s = 1/\{\alpha_{eff} c_1\} \approx 1$ ns, being c_1 the sound speed in corneal tissue), leads to rule out any pressure confinement during pulsed irradiation.

Some studies have reported measurements of these pressure peaks performed with piezoelectric foils attached on the rear surface of thin corneal layers or in models simulating tissues and structures of the ocular bulb [6,16,17]. The relevance of such studies from the clinical point of view is evident by considering the large number of patients subjected every year to excimer laser photorefractive keratectomy (PRK). In fact, even if as far as now this procedure appears impressively effective and safe, as confirmed by a significant follow-up time of a few years, many treatment techniques and postoperative regimens are currently under investigation in an attempt to minimize the residual adverse effects, such as epithelial hyperplasia and stromal reactive response, potentially causing regression of effect or corneal scarring. In view of the expected mass diffusion and technical refinements of such a surgical practice, a thorough comprehension of some physical and biological aspects involved in UV photoablation is necessary. In particular, whenever procedure developments are directed to stronger vision corrections by using larger irradiation diameters or longer exposure times, the potential risk of photomechanical damages associated with the larger energy doses employed must be carefully evaluated.

In this respect, we considered it particularly important to perform direct measurements inside real eyeballs of the pressure peaks produced by ArF laser ablation in order better to simulate the clinical conditions of PRK. This was done in porcine eyes by using a needle hydrophone that was expected not to perturb significantly the distribution of the pressure waves. Particular attention was drawn to the analysis of propagation effects modifying the pulse shapes to achieve an estimation of local pressure transients at the level of the various structures crossed by the acoustic wave.

MATERIALS AND METHODS

Experiments were done with freshly enucleated porcine eyes (22–25 mm in diameter), maintained in saline solution at 4°C until tests were executed. The experimental setup is sketched in Figure 1. The ArF laser employed was a commercial surgical excimer laser (Apogee Summit Technology, Waltham, MA) operated at the typical conditions of PRK: 180 mJ/cm^2 fluence, 1–10 Hz repetition rate, 1 to 6.5 mm irradiation spot diameters. The measured pulse duration was 15 ns (FWHM). Laser-induced acoustic transients were detected by means of a PVDF needle-probe hydrophone (Imotec GmbH, Germany). The rise time of this probe had been previously verified to be not greater than 15 ns by detecting the acoustic profile produced by tightly focusing the ArF laser beam into gelatine. The hydrophone was directly connected to the high impedance input (1 MΩ, 10 pF) of a fast digital oscilloscope (Tektronix 520A, 500 MS, 500 MHz) by means of a 1-m-long coaxial cable. Pressure pulse shapes were recorded after

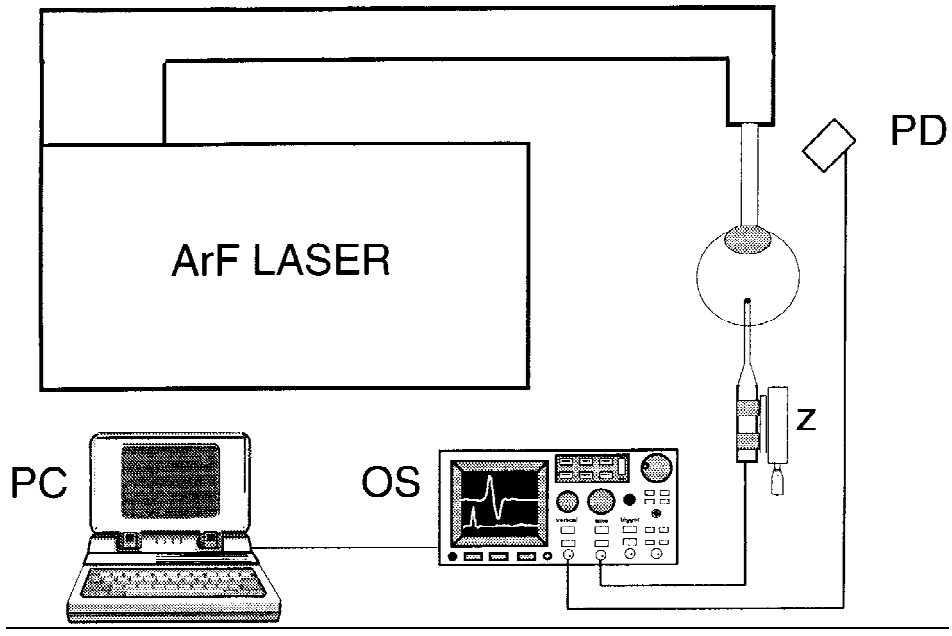

Fig. 1. Experimental setup. PD: fast photodiode, Z: micrometrical translation stage OS: oscilloscope, PC: portable computer.

each measurement by a portable computer. Considering that the acoustic transient is long with respect to the propagation time along the cable (5 ns), the lumped-constant network approximation can be assumed and the detected voltage pulse is simply proportional to the pressure pulse [18,19]. In this condition the sensitivity of the probe was of 2.54 mV/bar.

The hydrophone head (0.5 mm in diameter at the tip) was inserted into the ocular bulb from the posterior pole close to the macula and precisely advanced along the eye optical axis by means of a micrometric translation stage. In this way, the full bulb length could be scanned from retina to corneal endothelium to detect the evolution of pressure waves during their propagation. Moving toward the inner surface of the cornea, the lens was gently punctured and passed through by the probe.

Four series of measurements were performed with different diameters of the irradiated area: 6.5 mm, 5 mm, 3 mm, and 1 mm, respectively. For a given diameter, at each position of the probe along the eye axis, pressure values were determined by averaging over three acquisitions.

RESULTS

Acoustic Wave Speed

Recordings of the relative position of the needle probe into the eye allowed to evaluate the speed of the acoustic wave into the eyeball. The absolute position of the probe tip into the eye with respect to the cornea surface was derived by measuring the delay between the laser pulse (detected by a fast photodiode) and the pressure pulse, assuming a constant propagation speed of the acoustic wave corresponding to the value measured experimentally. This assumption appeared reasonably well verified, as shown in Figure 2, that reports a fitting of the wave motion measured for the 6.5 mm spot diameter, giving an average speed of (1570±15) m/sec. Similar values included in this uncertainty range also were found for the other irradiation diameters.

Pressure Peaks in the Anterior Chamber

Recorded data indicated that the pressure transient is always originated as a compressional positive peak, which was measured to be in the range of 55–90 bar in the anterior chamber, depending on the spot diameter (see Table 1). These values are in agreement with those observed under similar irradiation conditions on isolated corneal tissue samples [6,17]. The pulse duration of the positive peak was of ~50 ns FWHM in all the cases.

No distinct pulse originated by the thermoelastic response was ever observed beside the main peak due to tissue recoil. If any, it could not be temporally resolved by the hydrophone probe

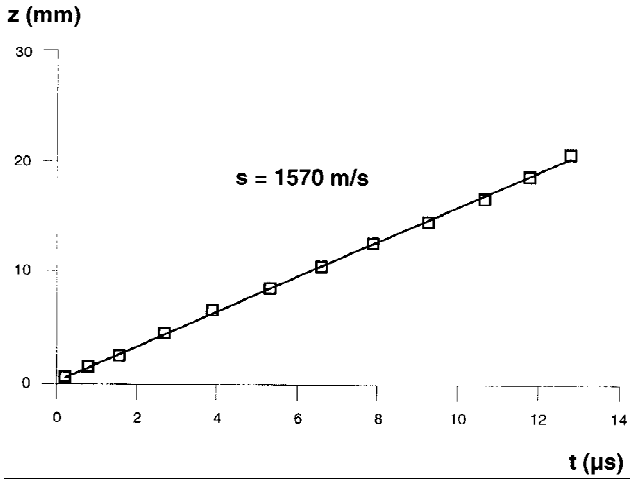

Fig. 2. Motion of the acoustical wave inside the eye and linear fitting to evaluate sound speed.

we used because of its short pulse duration (comparable with the stress relaxation time) and for the short time separation with respect to the more intense compressional peak associated with fast thermal explosion.

During our measurements we noted that the time shape and the amplitude of the pressure pulse were rather sensitive to the alignment of the needle probe relative to the optical axis, also in the vicinity of the cornea. However, pressure measurements fluctuations recorded at a fixed position of the probe were limited below 10%, being mostly due to energy fluctuations of the laser emission, without any significant perturbation in the pulse shape.

Propagation Effects

Experimental observations pointed out that the pressure pulse experiences significant diffraction and attenuation effects during propagation into the eye. Figure 3 shows an example of the pressure shape evolution for the 3 mm spot diameter, as recorded at increasing distances from the irradiated surface of the cornea. In all the series of our measurements with 6.5, 5, and 3 mm spot diameters, we noted that the original pressure shape presenting the only positive compression peak was modified during the propagation with the development of a marked rarefaction phase (evidenced by a negative peak following the positive one), which was found to reach its maximum on a propagation distance approximately equal to the laser spot diameter. In this condition, we recorded negative rarefaction peaks of 20–40 bar. For the 1 mm spot, the rarefaction phase was observed since the closest distance from to the irradiated surface (0.7 mm) that could be reached by the hydrophone tip, indicating that in this case the propagation through the thickness of the cornea was sufficient to develop observable diffraction effects (see Fig. 4). As an example of how propagation can affect the pressure pulse shape, we report in Table 1 the comparison among some pulse parameters, as measured in the anterior chamber close to the inner surface of the cornea and at the farthest propagation distance near the retina, respectively.

DISCUSSION

Pressure Pulse Evolution Modelling

We briefly summarize some key points of previously developed theoretical models providing the background for the analysis and the interpretation of the observed photoacoustic processes. The problem regarding the generation of laser-induced acoustic waves by superficial vaporization and their propagation into tissue is very complicated, and a general solution still awaited. Here, these two aspects of wave generation and propagation are regarded separately to simplify the picture.

Pulse generation. In the high intensity regime (10^7–10^8 W/cm^2), the "variable energy blast wave" theory allows quantitative estimation of the surface pressure time-history [20,21]. Assuming a fast vaporization and with reference to the irradiation conditions of this study, we can distinguish three distinct phases in the evolution of the pressure wave expanding outside the target in the air semi-space: (1) blast wave planar pumping while the laser is on, (2) planar decay, and (3) spherical decay.

The pressure on the surface of the target in the first phase while laser emission is still present is given by the expression:

$$p_{S1} = \left(\frac{\gamma+1}{2\gamma}\right)^{\frac{2\gamma}{\gamma-1}} \frac{\rho_0}{\gamma+1}\left[\frac{c_0^2 I_0}{p_0}\right]^{\frac{2}{3}} \qquad (1)$$

where I_0 is the laser intensity, $\gamma = c_p/c_v$ is the ratio of the specific heats of the surrounding gas, p_0, ρ_0, and c_0 are the imperturbed pressure, density, and sound speed of the gas, respectively. This equation indicates that the maximum pressure acting on the target surface scales as $I_0^{2/3}$. A similar behavior is provided also by another model

TABLE 1. Comparison Between Pressure Parameters*

Spot diameters [mm]	Measurements in anterior chamber[a]			Measurements near the retina[a]			
	P_+[b] [bar]	P_-[b] [bar]	Δt^+ [ns]	P_+[b] [bar]	P_-[b] [bar]	Δt_+ [ns]	Δt_- [ns]
6.5	76	4	50	24	15	66	210
5	86	7	47	19	9	72	174
3	90	9	50	9	6	70	110
1	55	21	50	1.2[c]	0.8[c]	45[c]	50[c]

*As measured inside the eye in the anterior chamber (at 0.5–1 mm from the irradiated corneal surface) and near the retina (at 20–22 mm from the corneal surface).
[b]P_+, P_-: compression and rarefaction peaks, respectively; Δt_+, Δt_-: time duration (FWHM) of positive and negative pulses, respectively.
[c]Weak signals at noise level.

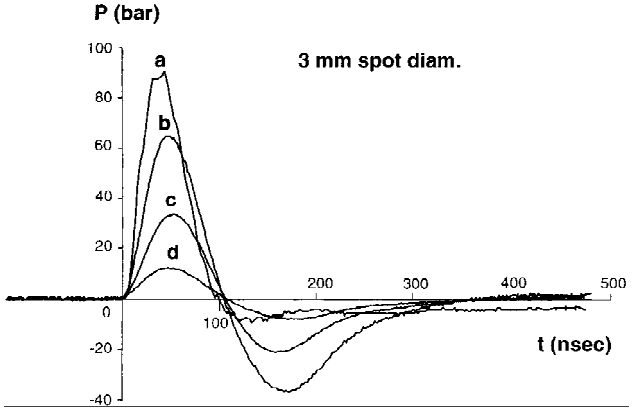

Fig. 3. Evolution of the pressure pulse shape during propagation along the eye optical axis. Spot diameter of 3 mm; sampling distance from the corneal surface: (**a**): 0.5 mm, (**b**): 5.7 mm, (**c**): 9.1 mm, (**d**): 19.5 mm.

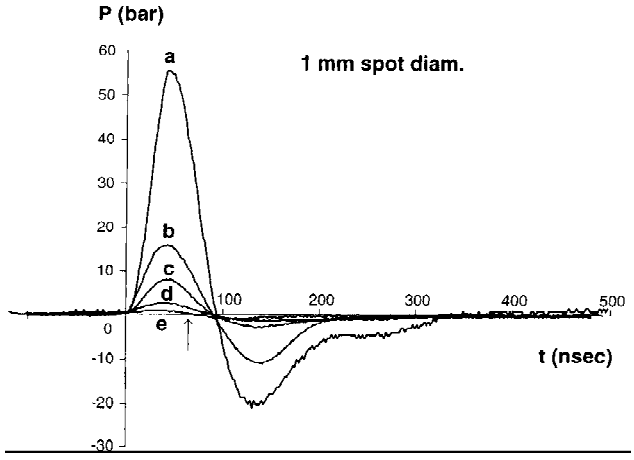

Fig. 4. Same as Figure 3, but for a spot diameter of 1 mm. Sampling distance from the corneal surface: (**a**): 0.7 mm, (**b**): 2.7 mm, (**c**): 5.7 mm, (**d**): 9.2 mm, (**e**): 21.6 mm. Curve (e) represents the far field pulse shape evidencing a sensible shortening of its duration (the arrow points the time width at the base of the positive peak).

that describes the stress generation via recoil of ablation products by assuming that the laser pulse heats a gas confined by two ideal pistons [22].

For the following phases corresponding to planar and spherical decay, one can derive similar expressions of the surface pressure, but characterized by different time dependences of the type $t^{-2/3}$ and $t^{-6/5}$, respectively. Fulfilling the continuity condition between consecutive stages, a complete pressure time history on the target surface can be obtained.

In Figure 5, we report an example of the evolution of the superficial pressure, calculated for $I_0 = 1.2\ 10^7$ W/cm^2 and irradiation diameter d = 1 mm. A peak pressure of ~50 bar and a pulse width $\tau_{ac} = 45$ ns were estimated. Similar behaviors can be derived for the other irradiation diameters, where the main difference with respect to Figure 5 is the time when the transition from planar to spherical decay occurs. Thus this simple model can provide some predictions about the shape of the generated pressure pulse and in particular can explain how a 15 ns laser pulse originates an acoustic pulse of longer time duration. However, as it is evident in Figure 5, this simplified model does not provide any numerical evaluation of the leading edge of the pressure pulse, which is determined by the true temporal envelope of the laser beam and by the vaporization dynamics.

By comparing these theoretical previsions with our experimental results, a good agreement can be found between the pulse width value τ_{ac} provided by vaporization model and the experimental one, which resulted in ~50 ns for all the spot diameters.

In contrast, the experimentally measured peak values are significantly higher. This underestimation suggests that the assumption of a complete vaporization postulated by this model is not acceptable. In fact, in agreement with the ablation dynamics hypothesized by other authors [6,16,23], it should be considered that the ejection of corneal materials occurs more likely as a cloud of water droplets including fragments of collagen and other proteins. The effect of this complex dynamics on the recoil pressure pulse generated into the bulk can be explained as a sort of confinement of the pressure wave expanding in the outer gas,

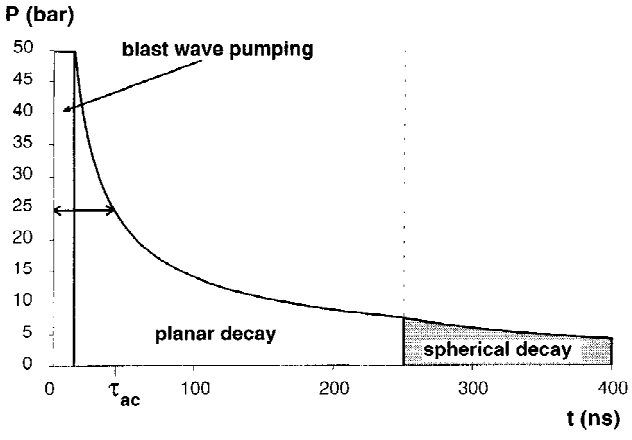

Fig. 5. Pressure time-history on the target surface as calculated from the "blast wave" model. τ_{ac} indicates the resulting pulse duration (FWHM).

because of the locally increased acoustic impedance due the presence of this aerosol. This process could enhance the peak pressure and justify the observation of higher values in comparison with theoretical previsions.

Pulse propagation. According to the blast wave model described above, under the condition d/2 >> Δz, where Δz is the axial length of the acoustic source, a plane wave will be generated whose front shape can be schematically represented by the curve in Figure 5. This wave will propagate inside the bulk at sound speed experiencing attenuation, diffraction, and scattering (nonlinear effects during propagation are negligible at the pressure levels here considered). A complete theoretical description of how these propagation effects can modify the acoustic pulse originated by tissue vaporization has not been given yet. Nevertheless some similarity with other models of acoustic wave propagation can help to obtain a qualitative interpretation of the observed behaviors, with particular concern to the development of the rarefaction phase.

In the specific case of thermo-optically excited acoustic pulses by laser radiation (typically occurring at energy densities well below the vaporization threshold), the problem of generation and bulk propagation of thermoelastic pulses has been theoretically solved by Karabutov and coworkers [24,25]. Their model describes diffraction effects due to geometrical and optoacoustic characteristics of the source, which have been well verified experimentally in many works [26–28] for various target materials. Regarding the generation of the pressure transient, two different types of pulse shape are expected, depending on the type of boundary at the irradiated surface. In case of a free boundary, the pressure pulse in the proximity of the target surface exhibits a double phase profile (compressional positive peak followed by a rarefaction negative peak produced by the reflection at the interface), whereas in the rigid boundary condition, only the compressional peak is present.

Considering this picture, one could compare the positive peak characterizing the thermoelastic response at a rigid boundary with the one originated by the recoil of ejected material in conditions of fast thermal explosion and assume that the propagation behavior of similar pulses can be qualitatively the same, despite their different physical origin. In details, modelling results, as well as experimental observations, indicate that the positive thermoelastic peak originated at a rigid boundary is modified during its propagation by diffraction effects that induce the formation of a rarefaction phase beside the compressional one. This propagation behavior is very similar to the one we observed for acoustic transients produced by ArF ablation of the cornea. It seem thus reasonable to argue that even in this last case, diffraction is responsible for the observed pulse shape modifications.

The diffraction of a plane acoustic wave is characterized in general by the diffraction parameter $D = z/L_D$, where z is the distance of the observation point along the optical axis from the acoustic source and L_D is the diffraction length:

$$L_D = \frac{d^2}{4\lambda_{ac}} \tag{2}$$

where λ_{ac} is the acoustic wavelength. D can be regarded as an acoustic parameter analogous to the inverse of the Fresnel number in optics. In the thermoelastic regime, λ_{ac} is determined by the penetration depth of optical radiation, whereas this is not true in the case of laser-induced fast vaporization. The blast wave model described above allows an estimation of $\lambda_{ac} = 2\ c_1\ \tau_{ac}$, and then of L_D (being c_1 the sound speed in the bulk). For example, for $d = 1$ mm one finds $L_D = 1.6$ mm, whereas for $d = 3$ mm, it results in $L_D = 14.3$ mm. This means that for irradiation spot diameters >1 mm, the acoustic wave behavior we observed after propagation over the full eye length was still the one typical of near field and acoustic Fresnel zone. Only for the 1 mm spot di-

ameter could we observe at the level of the retina some effect typical of far field propagation regime, such as a sensible decreasing of the duration of the pulse (see Fig. 4 and Table 1) whose shape tends to the derivative of the original positive pulse.

However, the distance over which diffraction effects typically produce substantial perturbation to the pulse shape can be much shorter than L_D. Karabutov et al. [26] observed relevant modifications to the profile of thermo-optically excited acoustical pulse (12 ns laser pulse duration) for a value of D as low as ~0.1 on the surface of a cupric chloride solution (absorbing coefficient of 50 cm^{-1}). In effect, also in the present work we recorded observable changes in the pulse shape due to diffraction for values of D of the same order of magnitude.

Pressure Peak Attenuation

Figures 6 to 9 show the behavior of both positive and negative pressure peaks as a function of the coordinate z as measured along the eye axis. Experimental data for 6.5, 5, and 3 mm spot diameters have been fitted with an exponential law of the type: $P(z) = P_0e^{-\alpha z}$ assuming a plane wave propagating in an absorbing medium, being α the damping coefficient depending on thermal dissipation and diffraction. Actually, this assumption is not strictly valid, but the fitting is done just to provide an empirical law for the attenuation of the pressure peak to be applied in the typical conditions of PRK. In the case of the smallest spot size (1 mm), the acoustic wave decay is better represented by a spherical rather than a plane wave, as evidenced in Figure 9, where experimental data are fitted by a law of the type $P(z) = A/z$. The damping coefficients calculated with the exponential fitting for the positive and the negative peaks indicated as α^+ and α^-, respectively, are reported in Table 2 together with the calculated value of the maximum pressure P_0. The attenuation coefficients appear to increase for decreasing spot diameters. This behavior is reasonably due to variations in the spatial characteristics of the generated waves that tend to become earlier spherical in case of smaller irradiation spots.

Clinical Implications to PRK

From a clinical point of view, the effect of the observed high pressure peaks on the delicate tissues and structures of the eye that are passed through by the travelling acoustic wave is still to be investigated and recognized. Nevertheless, the

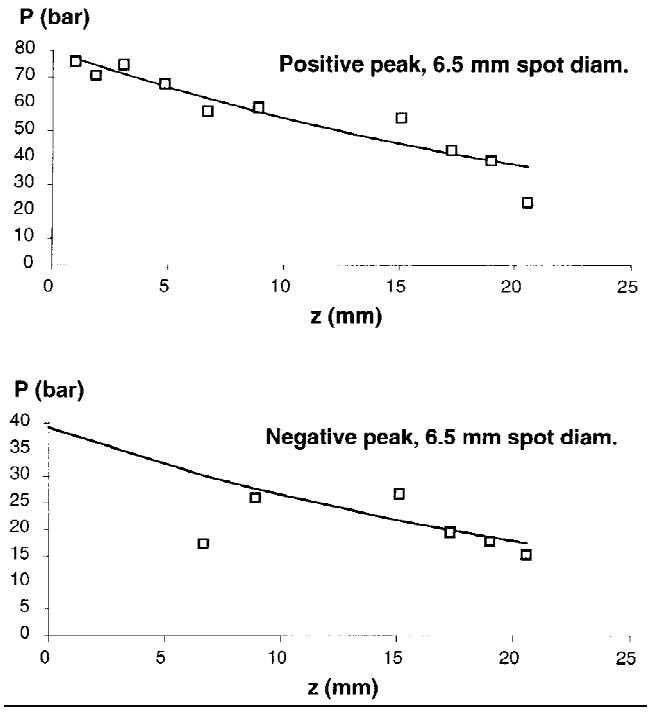

Fig. 6. Plane wave (exponential) fitting of the evolution of both positive and negative peaks for the irradiation diameter of 6.5 mm. The coordinate z is measured along the eye optical axis, from the corneal surface to the retina.

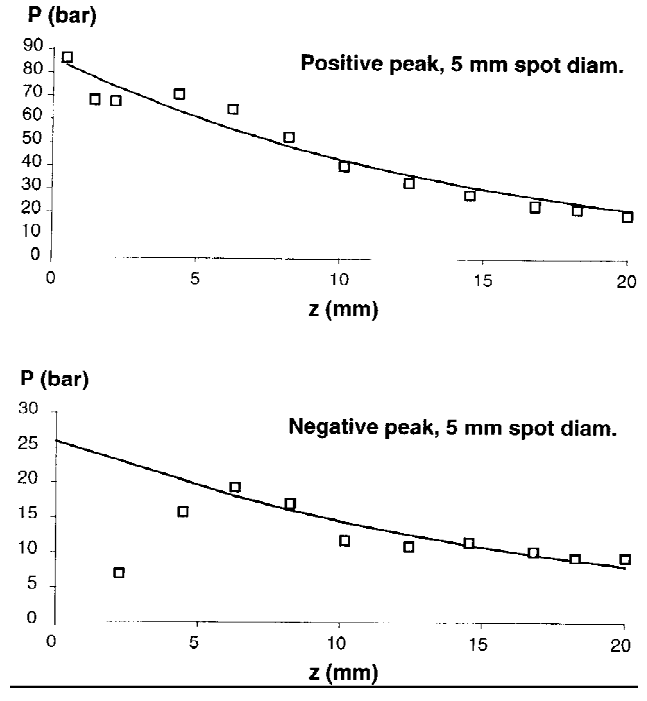

Fig. 7. Same as Figure 6, but for the irradiation diameter of 5 mm.

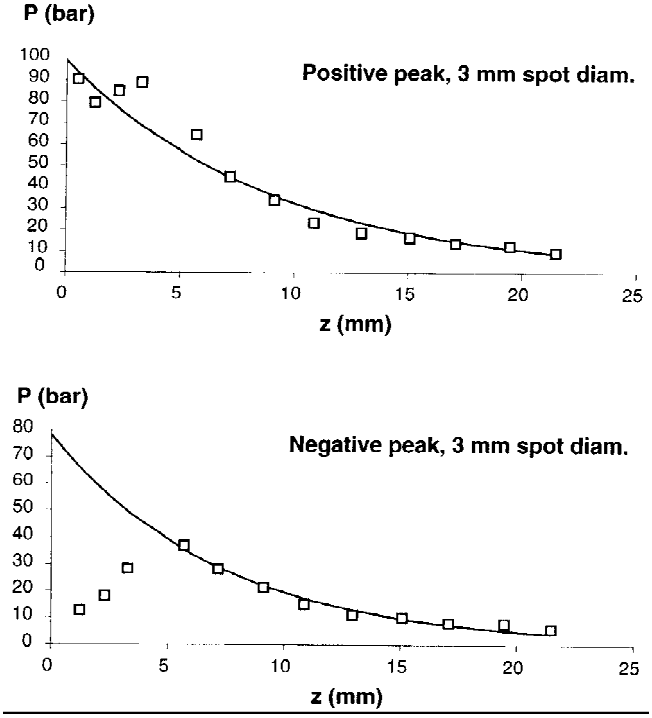

Fig. 8. Same as Figure 6, but for the irradiation diameter of 3 mm.

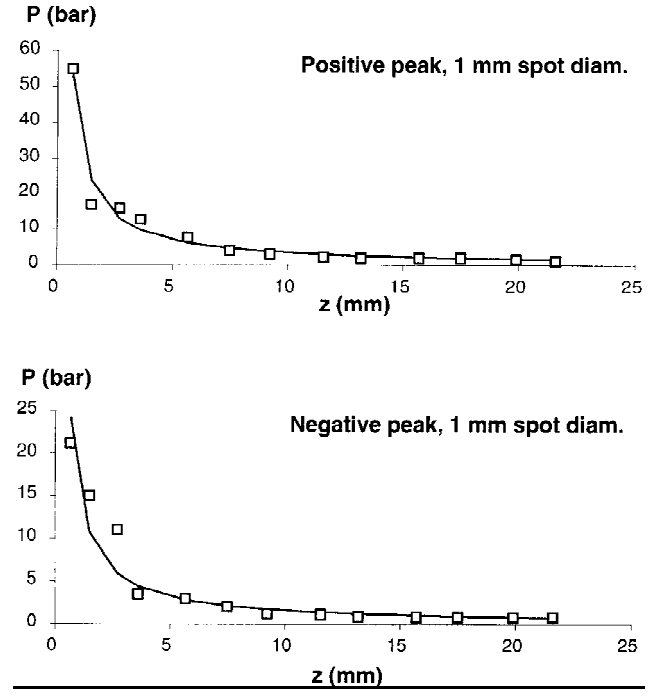

Fig. 9. Spherical wave (A/z type) fitting of the evolution of both positive and negative peaks for the irradiation diameter of 1 mm.

results of this study suggest some possible consequences to the PRK procedure that are worth discussing.

Despite ArF laser, fluence is usually kept constant during clinical applications for any irradiation diameter, originating compressional pulses of similar peak values, acoustic waves produced by larger diameters were found to experience a substantially lower attenuation, thus extending their effects on longer propagation distances, at least involving the retina. However, as suggested by clinical experiences in shock wave lithotripsy, compressional transients of 100 bars, 100 ns are expected to not significantly affect cellular morphology and functionality [29]. However, a major concern is represented by the observed growth of a rarefaction phase during pulse propagation, that is typically maximum on a distance similar to the irradiation diameter and can reach negative peak values of –40 bar. This effect could be responsible for local damages into tissue, as stretching, structural deformation, or even detachment of superficial layer cells, or at least induce cavitation bubble formations, being the threshold for these events as low as 10–20 bar in biological fluids [16].

With particular concern to the irradiation techniques clinically employed in PRK procedures, it must be noted that, according to our observations, the rarefaction effects can occur during the application of both the "full zone" static ablation technique and the "flying spot" scanning ablation technique. In the former case, an expanding diaphragm is used to modulate the laser beam cross section, typically from 0.5–1 mm up to 6–7 mm in diameter, to achieve the desired (myopic) correction. Thus the zone of potential damage from rarefaction waves progressively sweeps, as previously discussed, from the anterior chamber to the vitreous body and to the retina. In the second case, the laser beam is scanned over the corneal surface by keeping constant the irradiation diameter (typically in the range 0.5–1.5 mm) and the energy content. This means that the rarefaction pulse always develops in the anterior

TABLE 2. Calculated Parameters From Exponential Fittings of Peak Pressure*

Spot diameter [mm]	P_0[bar]	α^+[cm^{-1}]	α[cm^{-1}]
6.5	80	0.38	0.39
5	86	0.70	0.58
3	100	1.11	1.4

*P_0 is the maximum pressure, α^+ and α^- are the attenuation coefficients of positive and negative peak pressure values, respectively.

chamber, with repeated overlaps on the same points and with little or no attenuation due to the propagation.

CONCLUSIONS

Absolute measurements of the pressure transients induced by ArF laser pulses in typical conditions of PRK were performed in porcine eyes that represent an animal model very similar to the human eye. The recoil of ablated material from the corneal surface was found to originate compressional pressure pulses as high as 90 bar, in agreement with previous measurements in artificial samples. Moreover, our study on acoustic wave propagation inside the eye put in evidence a new feature, such as the development of a marked rarefaction phase, which was explained as a diffraction effect developing during pulse propagation. Also, original information on the acoustic wave speed and on the attenuation coefficients of both positive end negative peaks was obtained from real eye samples by numerical fitting of experimental data.

Further developments of this research will necessarily regard clinical studies on patients undergoing PRK, especially when larger irradiation diameters are employed. Specific investigations performed soon after laser surgery and in the follow-up will be aimed at identifying the presence of local injuries that could occur at different distances from the cornea, depending on the diameter of the irradiation spot, as suggested by the experimental observations of this work and by the propagation model discussed above.

REFERENCES

1. Trokel SL, Srinivasan R, Braren B. Excimer laser surgery of the cornea. Am J Ophthalmol 1983; 96:710–715.
2. Srinivasan R, Sutcliffe E. Dynamics of the ultraviolet laser ablation of corneal tissue. Am J Ophthalmol 1987; 103, Part II:470–471.
3. Dyer PE, Srinivasan R. Nanosecond photoacoustic studies on ultraviolet laser ablation of organic polymers. Appl Phys Lett 1986; 48:445–447.
4. Campbell EEB, Ulmer G, Bues K, Hertel IV. Analysis of ionic fragments from 308 nm photoablation of polyimide. Appl Phys A 1989; 48:543–547.
5. Puliafito CA, Steinert RF, Deutsch TF, Hillekamp F, Dehm EJ, Adler CM. Excimer laser ablation of the cornea and lens. Ophthalmology 1985; 92:741–748.
6. Srinivasan R, Dyer PE, Braren B. Far-ultraviolet laser ablation of the cornea: Photoacoustic studies. Lasers Surg Med 1987; 6:514–519.
7. Küper S, Brannon J, Brannon K. Threshold behavior in polyimide photoablation: Single-shot rate measurements and surface-temperature modeling. Appl Phys A 1993; 56:43–50.
8. Albagli D, Perelman LT, Janes GS, von Rosenberg C, Itzkan I, Feld MS. Inertially confined ablation of biological tissue. Lasers Life Sci 1994; 6:55–68.
9. Albagli D, Banish B, Dark M, Janes GS, von Rosenberg C, Perelman L, Itzkan I, Feld MS. Interferometric surface monitoring of biological tissues to study inertially confined ablation. Lasers Surg Med 1994; 14:374–385.
10. Esenaliev RO, Oraevsky AA, Letokhov VS, Karabutov AA, and Malinsky TV. Studies of acoustical and shock waves in the pulsed laser ablation of biotissue. Lasers Surg Med 1993; 13:470–484.
11. Dingus RS, Scammon RJ. Ablation of material by front surface spallation. In: Miller JC, Haglund Jr, RF, eds. "Laser Ablation, Mechanisms and Applications." New York: Springer-Verlag, 1991, pp 180–190.
12. Dörschel K, Müller G. Photoablation. In: Svaasand LO, ed. "Future Trends in Biomedical Applications of Lasers." SPIE, 1991, 1525:253–279.
13. Singleton DL, Paraskevopoulos G, Taylor RS. Dynamics of excimer laser ablation of polyimide determined by time-resolved reflectivity. Appl Phys B 1990; 50:227–230.
14. Ediger MN, Pettit GH, Weiblinger RP, Chen CH. Transmission of corneal collagen during ArF excimer laser ablation. Lasers Surg Med 1993; 13:204–210.
15. Ediger MN, Pettit GH, Hahn DW. Enhanced ArF laser absorption in a collagen target under ablative conditions. Lasers Surg Med 1994; 15:107–111.
16. Oraevsky A, Esenaliev R, Jacques S, Tittel F. Mechanism of precise tissue ablation with minimal side effects (under confined stress conditions of irradiation), In: Albrecht HJ et al., eds. "Laser Interaction with Hard and Soft Tissue II." SPIE 1994; 2323:250–261.
17. Kermani O, Lubatschowski H. Struktur und Dynamik photoakustischer Shockwellen bei der 193 nm Excimerlaserphotoablation der Hornaut. Fortschritte der Ophthalmologie 1991; 88:748–753.
18. Schoeffmann H, Schmidt-Kloiber H, Reichel E. Time-resolved investigations of laser-induced shock waves in water by use of polyvinylidenefluoride hydrophones. J Appl Phys 1988; 63:46–51.
19. Olmes A, Lohmann S, Lubatschowski H, Ertmer W. Correction of laser-induced pressure transient detected with PVDF-transducers. Appl Phys B (sub.), 1995.
20. Wu PK. Radiation-induced acoustic waves in water. AIAA J 1977; 15:1809–1811.
21. Pirri AN. Theory for momentum transfer to a surface with a high power laser. Physics of Fluids 1973; 16:1435–1440.
22. Zweig AD, Venugopalan V, Deutsch TF. Stress generated in polyimide by excimer-laser irradiation. J Appl Phys. 1993; 74(6):4181–4189.
23. Golovlyov VV, Letokhov VS. Laser ablation of absorbing liquids (acoustical microfragmentation mechanism). Appl Phys B 1993; 57:417–423.
24. Burmistrova LV, Karabutov AA, Portnyagin AI, Rudenko OV, Cherepetskaya EB. Method of transfer functions in problems of thermooptical sound generation. Sov Phys Acoust 1978; 24:369–374.
25. Karabutov AA, Rudenko OV, Cherepetskaya EB. Theory of the thermooptical generation of nonsteady acoustic fields. Sov Phys Acoust 1979; 25:218–224.

26. Karabutov AA, Portnyagin AI, Rudenko OV, Cherepetskaya EB. Experimental study of the propagation of short thermooptically excited acoustic pulses. Sov Phys Acoust 1980; 26:162–164.
27. Terzic M, Sigrist MW. Diffraction characteristics of laser-induced acoustic waves in liquids. J Appl Phys 1984; 56: 93–95.
28. Sigrist MW. Laser generation of acoustic waves in liquid and gases. J Appl Phys 1986; 60:R83–R121.
29. Pensel J, Thomas S, Lieck P, Barreton G. Analysis of tissue damage after laser induced shockwave lithotripsy. In: Steiner R, ed. "Laser Lithotripsy: Clinical Use and Technical Aspects." Berlin: Springer-Verlag 1988, pp. 77–81.